A Spring-Loaded Mechanism for the Conformational Change of Influenza Hemagglutinin

Chavela M. Carr and Peter S. Kim
Howard Hughes Medical Institute
Whitehead Institute for Biomedical Research
Department of Biology
Massachusetts Institute of Technology
Cambridge, Massachusetts 02142

Summary

Influenza hemagglutinin (HA) undergoes a conformational change that induces viral fusion with the cellular membrane. The structure of HA in the fusogenic state is unknown. We have identified a sequence in HA that has a high propensity for forming a coiled coil. Surprisingly, this sequence corresponds to a loop region in the X-ray structure of native HA: the loop is followed by a three-stranded, coiled-coil stem. We find that a 36 residue peptide (LOOP-36), comprising the loop region and the first part of the stem, forms a three-stranded coiled coil. This coiled coil is extended and stabilized in a longer peptide, corresponding to LOOP-36 plus the residues of a preceding, short α helix. These findings lead to a model for the fusogenic conformation of HA: the coiled-coil stem of the native state extends, relocating the hydrophobic fusion peptide, by 100 Å, toward the target membrane.

Introduction

Membrane fusion is necessary for a large number of diverse processes in biology. For example, protein trafficking, protein secretion, fertilization, and neurotransmission require the fusion of distinct membranes to form a single lipid bilayer. In general, membrane fusion is very slow in the absence of specific proteins.

The best-characterized membrane fusion event occurs in the infection of animal cells by influenza virus. Infection begins with the binding of virus to sialic acid, a component of membrane proteins and lipids. The bound virion is then internalized into a cellular endosome by receptor-mediated endocytosis. Ultimately, the viral envelope fuses with the membrane of the mature endosome in response to a drop in pH (for reviews see Wiley and Skehel, 1987; Stegmann and Helenius, 1993). Membrane fusion is promoted by the trimeric, viral-envelope glycoprotein, hemagglutinin (HA), which also functions in cell attachment by binding to sialic acid. At low pH, HA is sufficient for the fusion of membranes in vivo and in vitro (White et al., 1982a).

Each HA monomer is synthesized as a protein precursor, denoted HA0. The HA0 polypeptide is processed proteolytically to form a pair of disulfide-bonded peptides, denoted HA1 and HA2 (Lazarowitz et al., 1971; Skehel and Waterfield, 1975). This proteolytic processing is essential for the infectivity of the virus (Klenk et al., 1975; Lazarowitz

and Choppin, 1975). Native HA binds sialic acid, but is dormant for membrane fusion activity.

There is considerable evidence for a large, irreversible conformational change in HA that is required for membrane fusion (for reviews see Wiley and Skehel, 1987; White, 1992; see, however, Stegmann et al., 1990; Stegmann and Helenius, 1993). The conformational change is induced by mildly acidic conditions (e.g., pH ~5, the pH of the mature endosome) and results in a trimeric structure that is remarkably thermostable (Doms and Helenius, 1986; Ruigrok et al., 1986, 1988). At neutral pH, a similar conformational change, leading to a stable, fusion-active state of HA, can be induced at temperatures above 60°C (Ruigrok et al., 1986). The conformation of HA that is active for membrane fusion will be referred to as the fusogenic state.

Structure of the Native State of HA

HA can be proteolytically cleaved with bromelain to release the exoplasmic domain from the viral membrane. The resulting soluble domain, termed BHA, has sialic acid binding and low pH, liposome binding activities similar to those of intact HA (Brand and Skehel, 1972; Doms et al., 1985). The X-ray crystal structure of the BHA trimer, in the native state, has been determined with and without bound sialic acid (Wilson et al., 1981; Weis et al., 1988, 1990a). The interaction between HA and sialic acid has been well described (Weis et al., 1988; Glick et al., 1991; Sauter et al., 1992), and this interaction is separate from the membrane fusion activity of HA.

The central region of the HA2 polypeptide folds into a helical hairpin structure (see Figure 1a): a short α helix (red) is connected to a long α helix (magenta) by an extended loop region (yellow). The long α helix interacts with the corresponding long α helices from two other HA2 polypeptides to form an interwound rope of three helices, called a three-stranded coiled coil. The three shorter α helices are displayed on the outside of the coiled coil. The sialic acid–binding domains of the HA1 subunits assemble on top of the fibrous stem, which is formed primarily by the three-stranded HA2 coiled coil (Figure 1b). The length of the trimer, from the junction with the membrane to the distal tip of the HA1 subunits, is ~135 Å (Wilson et al., 1981).

HA2 is the transmembrane subunit, which spans the envelope membrane once. At the amino terminus of HA2 is a highly conserved, hydrophobic sequence of ~25 residues, known to be necessary for membrane fusion (Daniels et al., 1985; Gething et al., 1986a). Although buried in the hydrophobic interior in the native state (Figure 1, light blue), these residues become exposed in the fusogenic state (for reviews see Wiley and Skehel, 1987; Stegmann and Helenius, 1993) and insert into the endosomal membrane (Stegmann et al., 1991). For these reasons, this sequence is referred to as the fusion peptide (for a review see White, 1992).
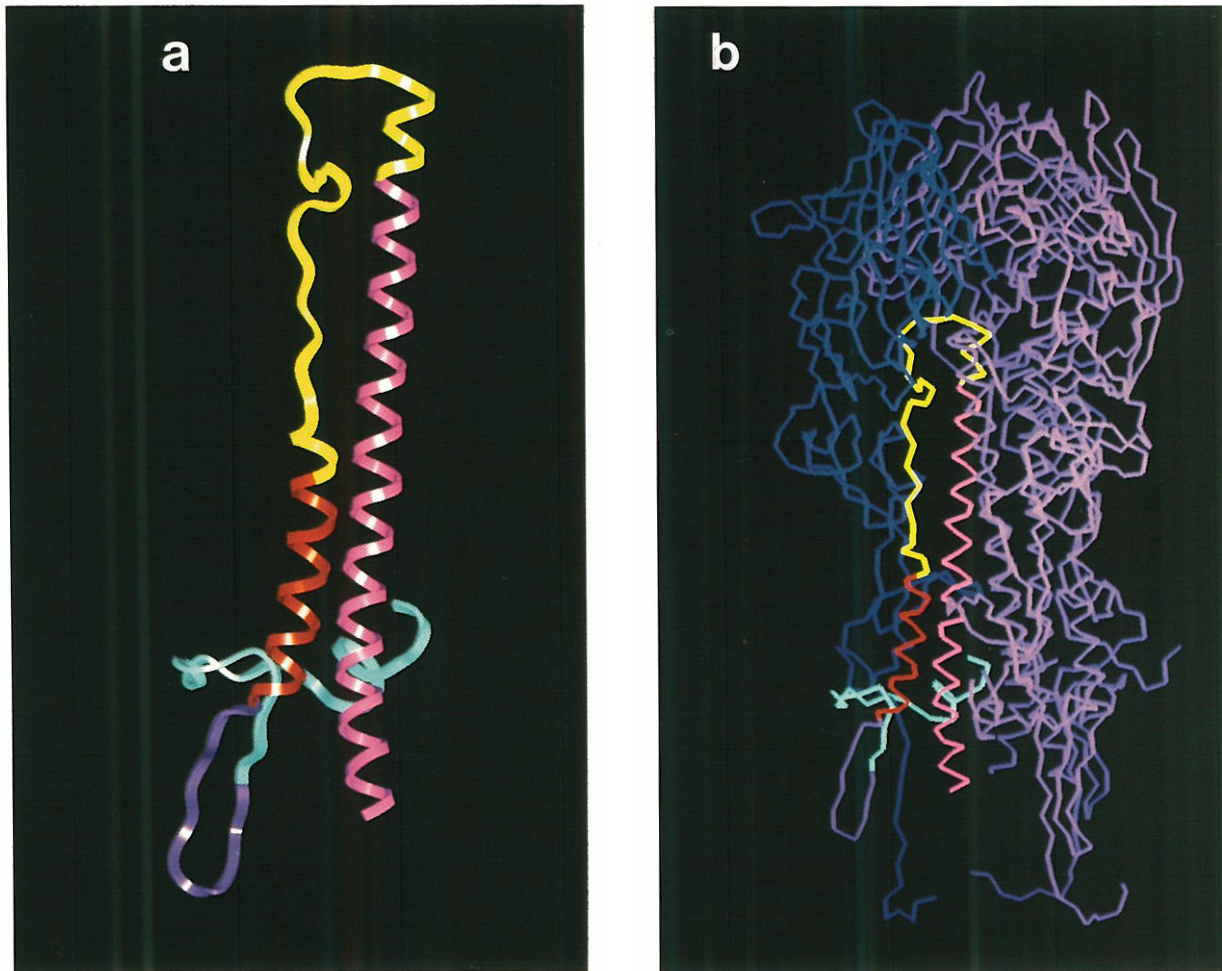
Figure 1. The Helical-Hairpin Structure in HA

The computer graphics representations are based on the crystal structure of bromelain-cleaved, native HA ectodomain, called BHA (Wilson et al., 1981; Weis et al., 1990a).

(a) A ribbon representation of the helical-hairpin structure in the transmembrane subunit (HA2) of HA. The C-terminal residues of HA2 are omitted for clarity. The N-terminal fusion peptide (light blue; residues 1–25) resembles a "hook," which is followed by a short antiparallel β sheet (purple; residues 26–37). The hook fastens two helices together in a helical-hairpin structure, which contains a short α helix (red; residues 38–53) connected to a long α helix (magenta; residues 82–125) by the loop region (yellow; residues 54–81). The long α helix associates with the corresponding long α helices of two other HA2 subunits, forming a three-stranded coiled coil (not shown).

(b) A backbone-trace representation of the interaction of the HA1 domain with the HA2 helical hairpin. The globular, sialic acid–binding domain (HA1) is at the top of the molecule. The viral membrane would be located at the bottom, and the target membrane of the endosome would be located at the top of the figure. The distance from the viral membrane to the distal tip of HA is 135 Å. The helical-hairpin structure of one HA2 subunit is colored as in (a); the C-terminal residues of HA2 are omitted, for clarity. The corresponding HA1 subunit is colored dark blue. The other HA monomers (purple) assemble to form a trimer, which buries the fusion peptides in the core of the coiled-coil interface.

The structure of HA in the fusogenic conformation is not known. An immediate puzzle is to understand how the exposed fusion peptide facilitates fusion of the viral envelope with the endosomal membrane, since, in the native conformation, the fusion peptide is buried near the viral envelope, ~100 Å from the distal tip of the HA molecule (Figure 1).

Model for the Structure of the Fusogenic State

We present a model for the fusogenic structure of HA. The model evolved from our interest in the coiled-coil motif found in many proteins (for a review see Cohen and Parry, 1990), including the leucine zipper domain of some transcription factors (Landschulz et al., 1988; O'Shea et al., 1989, 1991; Ellenberger et al., 1992). The coiled-coil motif consists of α helices wrapped around each other with a left-handed superhelical twist. In general, coiled coils contain either two (Crick, 1953) or three (Pauling and Corey, 1953) parallel α helices.

Coiled-coil sequences contain hydrophobic and hydrophilic amino acid residues in a repeating, heptad pattern (denoted positions a through g). Hydrophobic residues tend to occur at positions a and d of the heptad repeat, and these residues form the interface between helices.
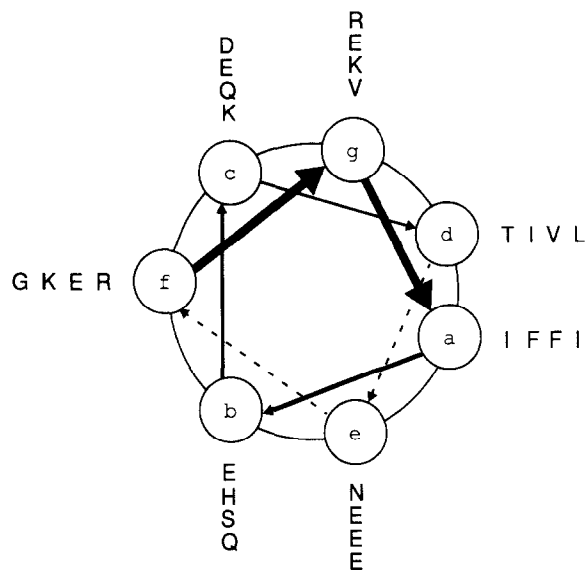
Figure 2. The Loop Region of the Helical Hairpin as a Coiled Coil

The 28 residues with high coiled-coil propensity (see Experimental Procedures) are projected onto a helical wheel. The view is down the helical axis starting at the N-terminus (position f). The alignment of predominantly hydrophobic amino acids at the a and d positions and the predominance of hydrophilic amino acids at other positions reveals the strikingly amphipathic nature of the sequence. Amino acid abbreviations: A, alanine; D, aspartic acid; E, glutamic acid; F, phenylalanine; G, glycine; H, histidine; I, isoleucine; K, lysine; L, leucine; N, asparagine; Q, glutamine; R, arginine; S, serine; T, threonine; V, valine; Y, tyrosine.

This feature is known as the 4-3 hydrophobic repeat and is a hallmark of coiled-coil sequences (Hodges et al., 1972; McLachlan and Stewart, 1975).

We evaluated the coiled-coil propensity for the amino

acid sequences of proteins with known three-dimensional structures. Segments of 28 residues were scored (Lupas et al., 1991) according to the statistical preference of different residues for a specific position in the heptad (Parry, 1982). This analysis (see Experimental Procedures) revealed a sequence in HA2 that has an unusually high score (Figure 2). Surprisingly, this high scoring region does not correspond to the known three-stranded coiled coil of HA but to the adjacent, extended loop region (Figure 1, yellow).

A closer examination of the HA2 sequence revealed a continuous, 88 residue sequence with the 4-3 hydrophobic repeat characteristic of coiled coils (Figure 3). The sequence begins at the N-terminus of the short α helix, includes the loop, and continues through the long α helix of the coiled coil (Figure 1, red, yellow, and magenta). The heptad repeat is maintained, in register, throughout the 88 residue region. This sequence is highly conserved among different strains of influenza virus (reviewed by Wiley and Skehel, 1987).

These considerations lead to the hypothesis that HA2 folds into a long, three-stranded coiled coil in the fusogenic state (Figure 4): the existing three-stranded coiled coil is extended to include the loop region and the short, external α helix. Thus, the 80 Å coiled coil that exists in the native state is extended to form a 135 Å coiled coil in the fusogenic state.

A protein conformational change of the magnitude proposed here, while rare, is not unprecedented. A striking example, demonstrated by X-ray crystallography, involves the serpin family of protease inhibitors. Upon cleavage of the reactive center peptide bond, a segment of these proteins can undergo a dramatic conformational change in secondary and tertiary structure, resulting in the reloca-
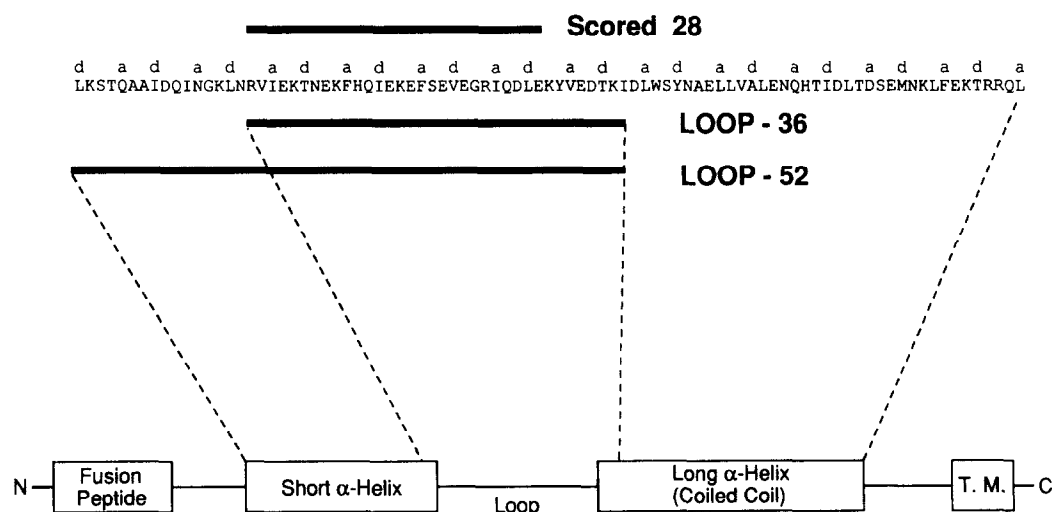

Figure 3. Position of the LOOP-36 and LOOP-52 Peptides in HA2

A schematic diagram of the structural units in the native structure of HA2. The 88 amino acid sequence (residues 38–125), proposed to form an extended coiled coil in the fusogenic state, is shown with the a and d positions of the heptad repeat indicated above the sequence. The high scoring, 28 residue region (residues 54–81) is indicated by a bar (Scored 28). The sequences of the LOOP-36 (residues 54–89) and LOOP-52 (residues 38–89) peptides are also indicated. LOOP-36 contains the entire loop region (residues 54–81) plus part of the sequence of the long α helix. LOOP-52 contains the entire short α helix plus the residues of LOOP-36. The fusion peptide is at the N-terminus, and the transmembrane region (T.M.) is near the C-terminus of HA2.
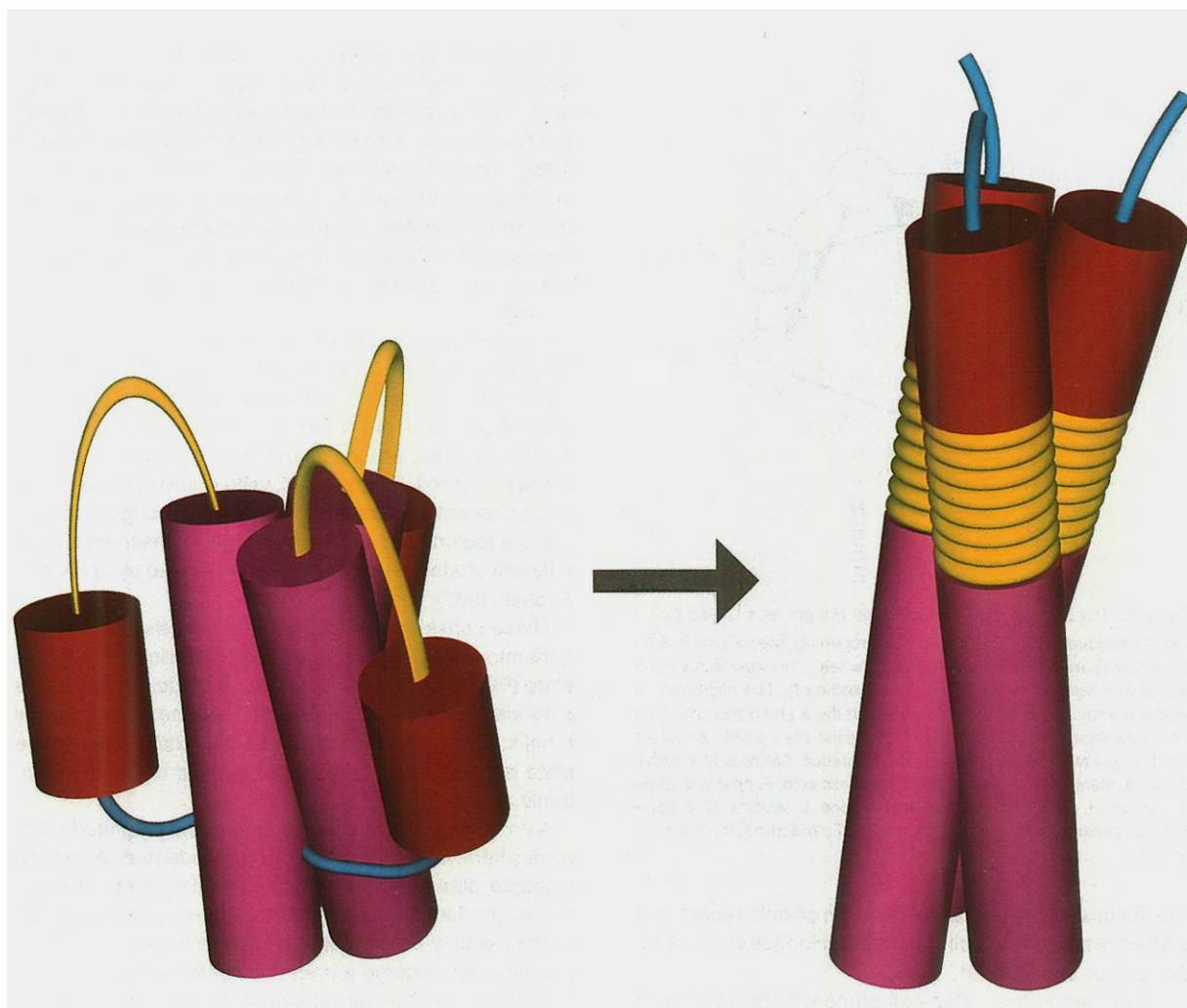
Figure 4. A Model for the Fusogenic State of HA

A trimer of HA2 molecules in the native state (left) is depicted schematically, as a stem of three helical hairpins (red, yellow, and magenta), each fastened by the N-terminal fusion peptide hook (blue), which is buried in the core of the coiled coil. In the fusogenic state (right), the HA1 subunits (not shown) are dissociated from the stem (see text), the fusion peptide is released from the protein interior, and the loop has "sprung" into a helical conformation to form an extended coiled coil that relocates the fusion peptide 100 Å toward the target membrane to promote membrane fusion.

tion of a short region by 70 Å (Wright et al., 1990; Stein et al., 1990; Mottonen et al., 1992). In addition, a conformational change with aspects similar to our model for HA has been proposed recently for the monomer to trimer transition of yeast heat shock factor (Rabindran et al., 1993).

Results and Discussion

To evaluate this model, we studied a 36 residue peptide called LOOP-36, which corresponds to the 28 residue loop region plus 8 residues of the long α helix (Figures 3 and 5A). Most short peptides do not fold into stable structures in aqueous solution (for reviews see Wright et al., 1988; Kim and Baldwin, 1990), although coiled-coil peptides containing four or five heptad repeats are a notable exception (Hodges et al., 1981; O'Shea et al., 1991). Thus, a stringent

test of the model is to determine if the LOOP-36 peptide forms a three-stranded coiled coil.

Although it is unfolded at neutral pH as determined by circular dichroism (CD) spectroscopy, LOOP-36 is highly helical (>90% at 100 μM) at pH 4.8 (Figure 5B). CD experiments also reveal a reversible thermal unfolding transition for LOOP-36 at pH 4.8 (Figure 5C). Sedimentation equilibrium experiments indicate that LOOP-36 is trimeric at pH 4.7 but primarily monomeric at pH 7.2 (Figure 5D). We conclude that LOOP-36 folds into a trimeric, α-helical coiled coil at the pH of membrane fusion.

There is a dramatic change in the α-helical CD signal of LOOP-36 between pH 5 and pH 7 (Figure 5E). The predominance of acidic residues at particular heptad positions in the LOOP-36 sequence (see Figure 5A) is reminiscent of the arrangement seen in the Fos leucine zipper homodimer, which displays a similar pH dependence of
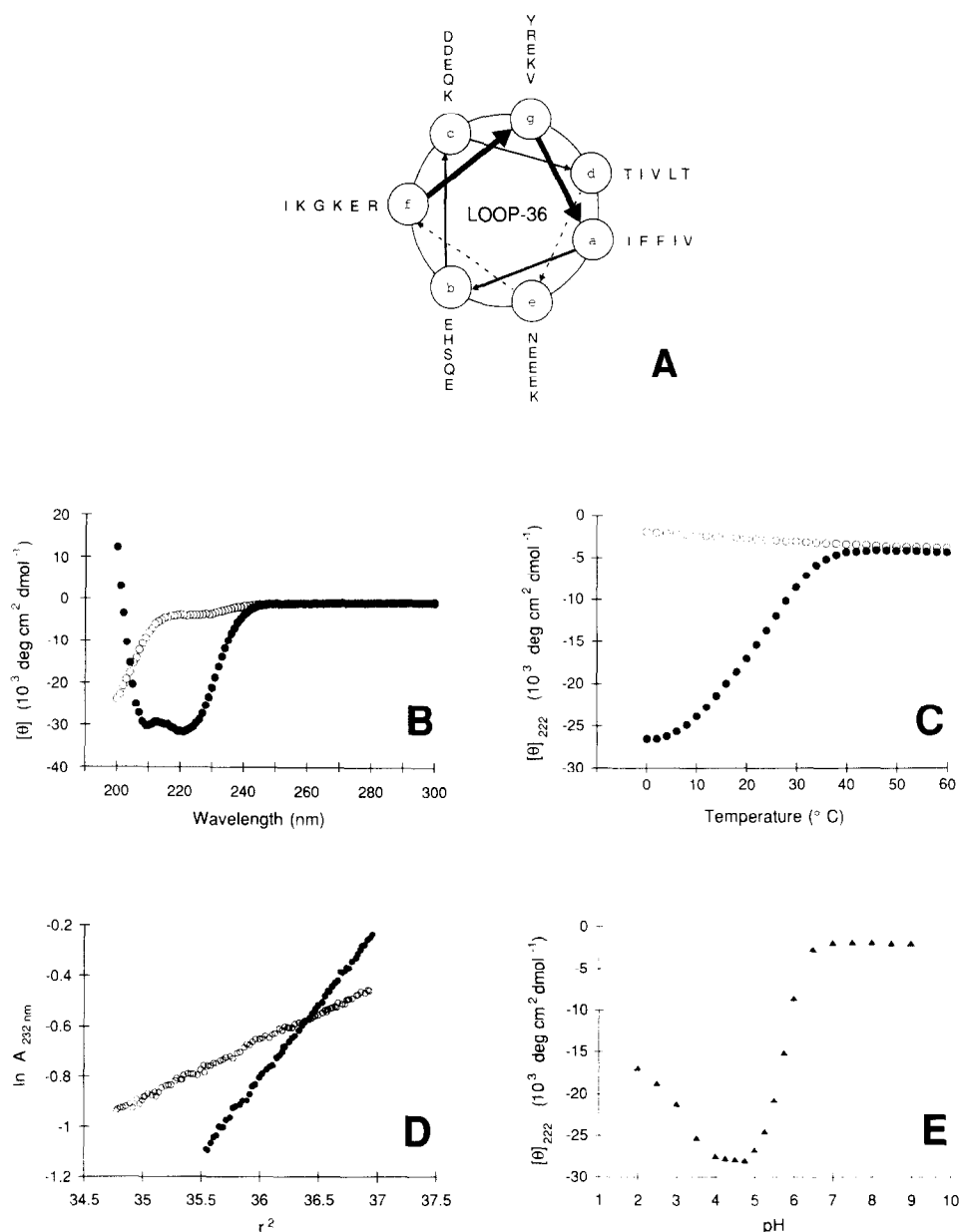
Figure 5. Folding of LOOP-36 as a Helical Trimer

LOOP-36 at neutral pH (open circles) and low pH (closed circles).

(A) LOOP-36 as a coiled coil. The sequence of the LOOP-36 peptide is projected onto a helical wheel, as in Figure 2.

(B) CD spectroscopy at 0°C indicates a characteristic α-helical spectrum (>90% helix content based on the value of $[\theta]_{222}$) for LOOP-36 at pH 4.8. The CD spectrum for LOOP-36 at pH 7.0 indicates a random-coil conformation.

(C) The CD signal at 222 nm for LOOP-36 shows a cooperative, thermal-unfolding transition at pH 4.8. No transition is seen for LOOP-36 at pH 7.0.

(D) The molecular mass of LOOP-36, as determined by sedimentation equilibrium experiments. The slopes of the data shown are proportional to molecular weight (see Experimental Procedures). For LOOP-36, the average molecular mass at pH 4.7 was 13.6 kd (expected mass for trimer was 13.4 kd), while the measured molecular mass at pH 7.2 was 5.2 kd (expected mass for monomer was 4.5 kd).

(E) The pH dependence of helix content in LOOP-36. The CD signal at 222 nm (closed triangles) is monitored by CD spectroscopy at 0°C as a function of pH. Helix content is highest between pH 4 and 5.

stability (O'Shea et al., 1992). Protonation of acidic side chains at low pH alleviates electrostatic repulsion that destabilizes the folded conformation at neutral pH. There is a second structural transition seen for LOOP-36 at even lower pH (Figure 5E), but the conformation at pH 2 probably is not relevant for membrane fusion.

Nonetheless, the coiled coil formed by LOOP-36 is not very stable, even at pH 5 (Figure 5C). In addition, as mentioned earlier, the fusogenic conformation of HA can be induced at neutral pH with elevated temperature. We therefore suspected that coiled-coil structure in the loop region would be stabilized in the context of the longer
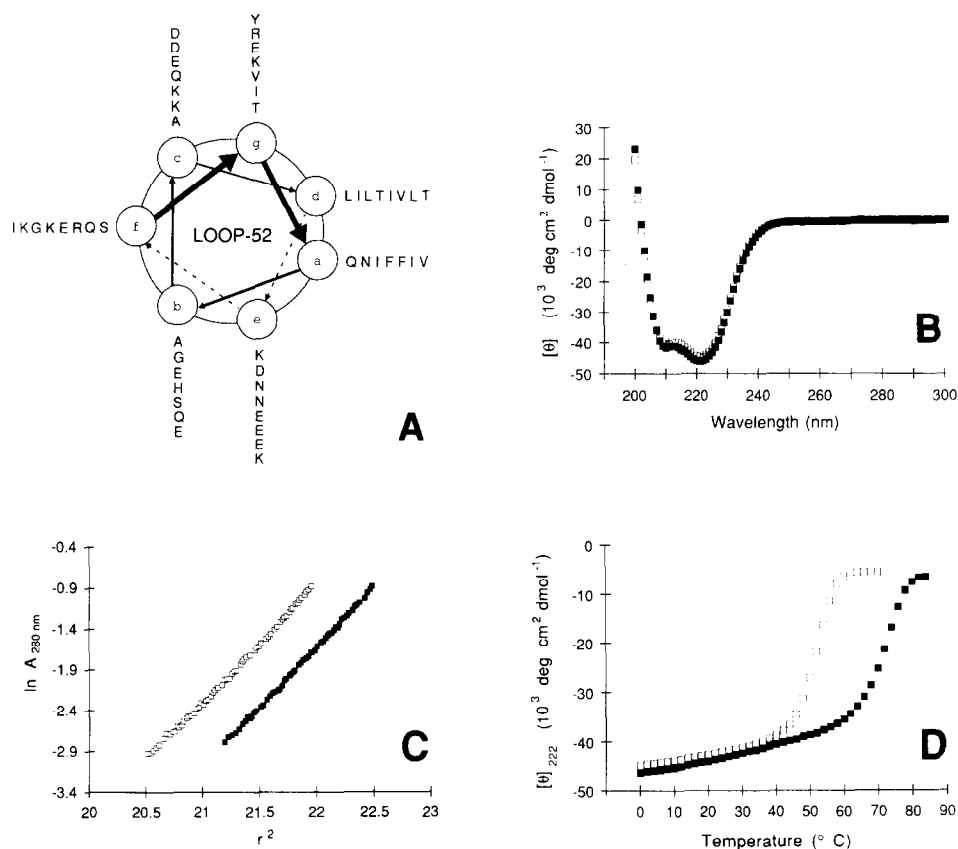
Figure 6. Folding of LOOP-52 as a Helical Trimer

LOOP-52 at neutral pH (open squares) and low pH (closed squares).

(A) LOOP-52 as a coiled coil. The sequence of the LOOP-52 peptide is projected onto a helical wheel, as in Figure 2.

(B) CD spectroscopy studies of LOOP-52 (0°C) indicate characteristic α-helical spectra ($\sim$100% helix content) at pH 4.8 and at pH 7.0. The value of $[\theta]_{222}$ for 100% helicity in peptides of this length is thought to be approximately $-40,000$ degrees $cm^2 \, dmol^{-1}$ (Chen et al., 1974).

(C) The molecular mass of LOOP-52, as determined by sedimentation equilibrium experiments. The average molecular masses for LOOP-52 were 18.4 kd at pH 4.7 and 19.5 kd at pH 7.2 (expected mass for trimer was 18.4 kd).

(D) The CD signal at 222 nm for LOOP-52 shows a cooperative, reversible, thermal-unfolding transition, at both pH 4.8 ($T_m = 72°C$) and pH 7.0 ($T_m = 52°C$).

coiled coil. To test this notion, we studied a 52 residue peptide, LOOP-52, which begins at the N-terminus of the short α helix and ends at the C-terminus of LOOP-36 (Figures 3 and 6A).

LOOP-52 forms a fully helical ($\sim$100%) structure at pH 7.0 and pH 4.8 (Figure 6B). At both neutral pH and pH 4.7, LOOP-52 is a trimer, as determined by equilibrium sedimentation (Figure 6C). The trimeric, helical structure in LOOP-52 is very stable: at pH 7.0, LOOP-52 unfolds with a transition midpoint (T_m) of 52°C, and at pH 4.8, the T_m is 72°C (Figure 6D).

Comparison with Other Results

It is extremely unusual for a small protein fragment, in aqueous solution, to fold into a stable structure that is different from that found in the native protein. Our results indicate that the loop region can fold as a three-stranded coiled coil; provide strong support for the proposal that, in the fusogenic state, the coiled coil includes the external

α helix in addition to the loop region; and indicate that the longer coiled coil is very stable, even at neutral pH.

Consistent with our model for the conformation of the fusogenic state, HA is trimeric at pH 5 (Doms and Helenius, 1986). In addition, electron microscopy studies suggest that an extended fibrous structure is formed on the surface of influenza viral membranes, following treatment at low pH or elevated temperatures at neutral pH (Ruigrok et al., 1986, 1988).

Earlier proteolysis experiments provide strong biochemical support for our model. Although certain regions of the fusogenic state of HA are sensitive to proteolysis, much of the HA2 subunit is resistant to degradation (Skehel et al., 1982; Ruigrok et al., 1988). The final tryptic digestion product of HA2 starts at residue 40, and that obtained with thermolysin starts at residue 38. In both cases, the residues of the short α helix, loop region, and the long α helix remain intact. The native state of HA is resistant to proteolysis. Nonetheless, if HA2 maintained the helical hairpin structure in the fusogenic state, one would expect
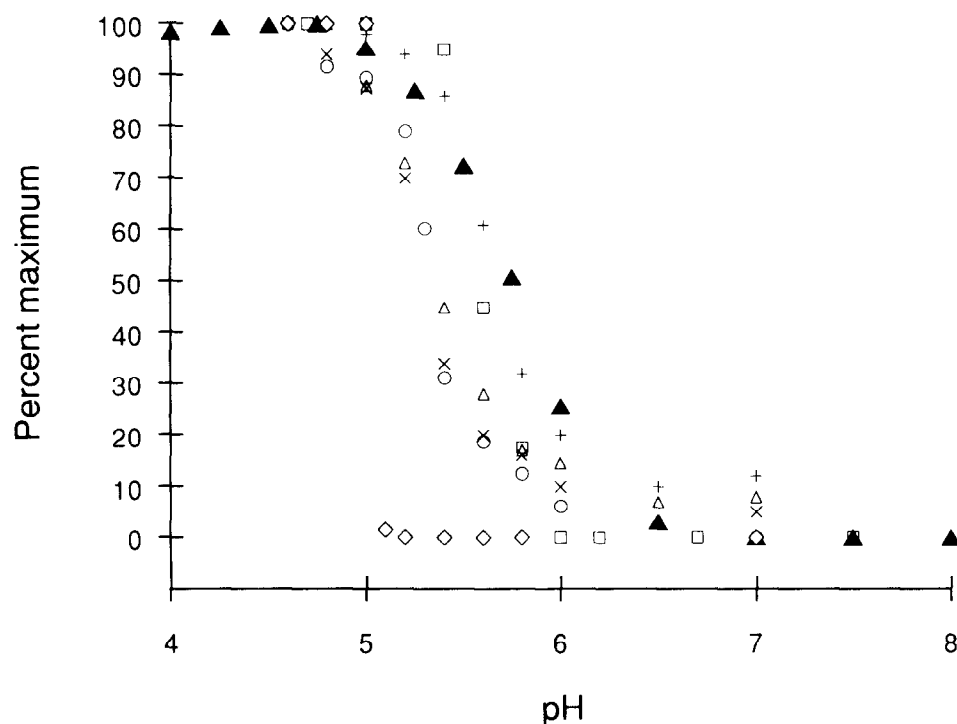
Figure 7. The LOOP-36 Folding Transition Occurs in a Physiologically Relevant pH Range

Normalized CD data for LOOP-36 (closed triangles; from Figure 5E) are superimposed on published results for the pH transitions of HA conformational change and membrane fusion activity. The transition at ~pH 5.7 for the CD data agrees well with other pH transitions reported for HA. A sharp transition is seen between pH 7 and pH 5 for viral-cellular membrane fusion (open squares) (Wharton et al., 1986), exposure of a fusion peptide epitope to a monoclonal antibody (plus signs) (White and Wilson, 1987), protease sensitivity of BHA (open circles) (Doms et al., 1985), liposome binding by BHA (exes) (Doms et al., 1985), dissociation of HA1 subunits and exposure of an epitope to a monoclonal antibody (open triangles) (White and Wilson, 1987), and cell–cell fusion by virus particles (open diamonds) (Doms et al., 1985).

the loop region to be sensitive to proteolysis upon dissociation and degradation of the HA1 subunits. In contrast, protection from proteolysis would be expected for the loop region if it were part of a coiled coil, as in our model.

Mechanism of the Conformational Change

One hypothesis for the mechanism of the conformational change is that a decrease in pH shifts the thermodynamic equilibrium between the native and fusogenic states. It is striking that the following pH transitions coincide: LOOP-36 helicity (and LOOP-52 stability), the known pH dependences for the conformational changes, and the onset of membrane fusion activity in HA (see Figure 7). All of these transitions occur abruptly between pH 7 and pH 5. If the mechanism for the conformational change is under thermodynamic control, it may be possible to design fusion mutants that alter the stability of the long coiled coil, and hence the fusogenic state, without affecting the stability of the native state.

For several reasons, however, we favor a kinetically controlled mechanism for the conformational change in HA, in which the native state of HA is metastable (i.e., although it is stably folded, it has the potential to form a thermodynamically more stable state). First, the conformational change, induced either by a decrease in pH or by an increase in temperature at neutral pH, is irreversible (Ruigrok et al., 1986; for reviews see Wiley and Skehel, 1987;

Stegmann and Helenius, 1993). Second, since LOOP-52 is very stable, even at neutral pH (Figure 6D), we expect that the 88 residue coiled coil of the fusogenic conformation will be extremely stable at both low and neutral pH. Third, an analysis of HA fusion mutants, obtained in a genetic selection, shows a striking correlation between the increase in the pH of fusion and the decrease in the temperature of fusion at neutral pH (Ruigrok et al., 1986), suggesting that the mutations destabilize the native state.

In addition, previous biophysical studies provide strong evidence for a mechanism that is under kinetic control. CD experiments with HA fragments reveal an irreversible thermal transition at ~63°C, correlated with the temperature of HA-mediated fusion at neutral pH, followed by a second, reversible transition at an even higher temperature (Ruigrok et al., 1986; see, however, Ruigrok et al., 1988). The irreversibility of the first transition is consistent with a transition from a metastable initial state to a more stable final state. We would assign the second transition to the unfolding of the long, stable coiled coil.

The notion of a metastable structure raises the question: how does HA fold into a conformation that is not the most thermodynamically stable structure? The in vivo folding of the HA0 precursor is known to be ATP dependent (Braakman et al., 1992). A minority of the HA0 molecules fail to fold into the native conformation, but instead form stable, aberrant trimer species that do not leave the endo-

plasmic reticulum (Gething et al., 1986b; Copeland et al., 1986). These species may have an extended coiled-coil structure similar to our proposed fusogenic conformation. Thus, the native conformation of HA may be the result of the in vivo folding pathway of the HA0 precursor. In addition, the relative instability of the loop region of HA2 at neutral pH (see Figure 5C) may be important for in vivo folding of HA0.

Regardless of whether the mechanism is under thermodynamic or kinetic control, there appear to be two types of interactions that stabilize the native state and thereby inhibit formation of the fusogenic state: intersubunit HA1 protein–protein interactions and burial of the fusion peptide in the hydrophobic core of the trimer. As mentioned previously, in the fusogenic conformation the HA1 subunits have dissociated and the fusion peptide is exposed (see, however, Stegmann et al., 1990; Stegmann and Helenius, 1993).

In the structure of the native state, extensive interactions are apparent (Wilson et al., 1981) between the loop region of HA2 and its corresponding HA1 subunit (see Figure 1b). Thus, the HA1 subunit may act as an inhibitor or "clamp" that binds to the loop region, preventing the conformational change. In addition, multiple HA1–HA1 interactions are likely to inhibit the conformational change. Indeed, introducing disulfide bonds between HA1 subunits prevents the conformational change in HA and inhibits membrane fusion activity (Godley et al., 1992). Furthermore, many mutations that alter the pH of fusion appear to destabilize HA1–HA1 or HA1–HA2 interactions in the native state (reviewed by Wiley and Skehel, 1987).

The native conformation may also be stabilized by the fusion peptide, which makes significant hydrophobic interactions in the core of the native structure. The buried fusion peptide resembles a hydrophobic "hook," which holds the helices together in a helical-hairpin conformation (see Figure 1a). Many of the HA mutants that fuse under less acidic conditions (Daniels et al., 1985; Gething et al., 1986a) contain amino acid substitutions near the region of the fusion peptide. For example, the X-ray crystal structure of the HA2 fusion mutant, D112G, indicates that four hydrogen bonds are lost (per monomer) between the aspartate side chain and residues of the fusion peptide. The pH of fusion for the mutant is elevated by 0.4 pH units, presumably because loss of the hydrogen bonds destabilizes the native state (Weis et al., 1990b).

Speculation on the Relevance to Other Fusion Events

Although influenza HA is the best-characterized membrane fusion protein, other viral (and nonviral) fusion proteins are known to be oligomeric (reviewed by White, 1992), and some of these are candidates for further study in light of our model. Like HA, these glycoproteins are derived proteolytically from a precursor; this proteolysis creates a new N-terminus with an adjacent fusion peptide sequence (for reviews see White, 1990; Stegmann and Helenius, 1993). Moreover, several of these fusion peptide sequences are followed by a stretch of amino acids with a 4-3 hydrophobic repeat, suggesting a coiled-coil structure

(Chambers et al., 1990). Our results suggest that some of these 4-3 hydrophobic repeat sequences may fold into different conformations in the native and fusogenic states of the glycoprotein.

Proteins that mediate fusion at neutral pH (for example, those involved in fertilization, protein trafficking, or human immunodeficiency virus [HIV] infection; reviewed by White, 1992) may also unleash a latent fusogenic conformation in response to an external stimulus, such as binding of a receptor or interaction with another protein. For example, the binding of HIV to CD4 is known to induce conformational changes in the envelope glycoprotein that result in release of the extracellular subunit (gp120) from the transmembrane subunit (gp41), exposure of the fusion peptide, and fusion of the viral membrane with the cell (reviewed by Vaishnav and Wong-Staal, 1991). A peptide from gp41, corresponding to a sequence adjacent to the N-terminal fusion peptide, has been shown to form a coiled coil (Wild et al., 1992). Moreover, expression of gp41 in the absence of gp120 results in syncytium formation (Perez et al., 1992), demonstrating that the interaction between gp120 and gp41 inhibits fusion activity, possibly in a manner similar to our proposed inhibitory interaction of the HA1 and HA2 subunits in the native state of HA.

Finally, if our model is correct, it may lead to new insights for the discovery of anti-viral drugs. For example, therapeutic agents might be designed to prevent the low-pH activation of HA (Wiley and Skehel, 1987; Godley et al., 1992; Kemble et al., 1992). Alternatively, since acid pretreatment of influenza virus can abolish infectivity (e.g., White et al., 1982b; Puri et al., 1990) agents might be designed that cause the conformational change to occur prematurely (Wiley and Skehel, 1987). It is also interesting, in light of our results, that a synthetic coiled-coil peptide from gp41 of HIV inhibits viral replication (Wild et al., 1992).

Experimental Procedures

Coiled-Coil Prediction
An algorithm (Parry, 1982) was used to predict coiled-coil propensities based on the statistical preference of different amino acids for each position in the heptad repeat. Sequences from the Protein Data Bank (Brookhaven) were analyzed using a computer program ("coiledcoil;" Lupas et al., 1991) based on the algorithm. With a window size of 28 residues, sequences with scores above 1.3 are thought to have a high probability of being coiled-coil structures, while scores between 1.1 and 1.3 generally correspond to amphipathic α helices in globular proteins (Lupas et al., 1991). A score of 1.6 was obtained for residues 54–81 of HA2. For comparison, a score of 1.9 was obtained for the GCN4 leucine zipper sequence.

Inspection of the complete HA2 sequence revealed a continuous heptad repeat from residues 38 to 125. Although an earlier analysis had predicted a coiled-coil structure for much of the 88 residue sequence of HA2 identified here, the register of the heptad repeat was not maintained throughout this sequence, and several interruptions in the coiled coil were also predicted (Ward and Dopheide, 1980; see also Chambers et al., 1990).

Peptide Synthesis and Purification
Peptides were synthesized on an Applied Biosystems model 430A peptide synthesizer using Fmoc chemistry with Fastmoc reaction cycles modified to include acetic anhydride capping (Fields et al., 1991). LOOP-36 corresponds to residues 54–89, and LOOP-52 corresponds to residues 38–89 of HA2 from the X-31 strain of influenza virus (Kilbourne, 1969). In each peptide, the N-terminus is acetylated and the

C-terminus is amidated. The peptides were cleaved using standard Fmoc protocols and desalted on a Sephadex G-10 or G-25 column (Pharmacia) in 5% acetic acid. Final purification was by reverse-phase, high performance liquid chromatography (Waters, Inc.) at 25°C using a Vydac preparative or semipreparative C18 column (stock numbers 218TP1022 or 218TP510, respectively). A linear acetonitrile–water gradient of 0.1% buffer B increase per minute was used with a flow rate of 10 ml/min (5 ml/min for the semipreparative column). Buffer A is 0.1% trifluoroacetic acid in water; buffer B is 90% acetonitrile and 0.1% trifluoroacetic acid in water. The identity of the peptides was confirmed by laser desorption mass spectrometry (Finnigan MAT LA-SERMAT). The measured mass for LOOP-36 was 4451 daltons (expected 4450 daltons), and the measured mass for LOOP-52 was 6147 daltons (expected 6146 daltons).

CD Spectroscopy

CD experiments (for a review see Woody, 1985) were performed on an AVIV CD spectrophotometer (model 62DS) equipped with a thermoelectric temperature controller. The cuvettes used for thermal unfolding studies and pH studies were 1 cm and 0.1 mm in pathlength, and the cuvettes used for wavelength spectra were 1 mm and 0.1 mm in pathlength. Peptide concentration was determined by tyrosine absorbance at 275.5 nm (Edelhoch, 1967) in 6 M guanidinium chloride (Schwarz/Mann Biotech, Ultra-Pure grade).

The pH dependence of LOOP-36 structure was determined by monitoring the CD signal at 222 nm. Measurements were made at 0°C and 32 mM peptide in a buffer of 150 mM sodium chloride, 20 mM (each) sodium borate, sodium citrate, and sodium phosphate. Both transitions observed in the pH dependence studies are >95% reversible (data not shown).

For thermal unfolding experiments, the CD signal was monitored at 222 nm as a function of temperature. Samples at pH 7.0 contained 32 μM LOOP-36, 10 mM sodium phosphate, and 150 mM sodium chloride; or 500 μM LOOP-52, 50 mM sodium phosphate, and 150 mM sodium chloride. Samples at pH 4.8 contained 10 mM sodium citrate, 10 mM sodium phosphate, and 10 mM sodium borate for both LOOP-36 and LOOP-52. All thermal unfolding experiments are reversible (>95% for LOOP-36 samples and >85% for LOOP-52 samples) in the temperature range from 0°C to 60°C for LOOP-36 and 0°C to 85°C for LOOP-52 (data not shown).

CD spectra were obtained at 0°C, in the same conditions as used in thermal unfolding experiments, except that the peptide concentration was 100 μM for LOOP-36. In Figure 7, percent helicity for LOOP-36 was calculated assuming that 100% helicity corresponds to −33,000 degrees cm^2 dmol^{-1}, as has been found in studies of helical peptides of this length (Chen et al., 1974).

Equilibrium Sedimentation

Molecular weights were determined, at 1°C for LOOP-36 and 25°C for LOOP-52, by analytical ultracentrifugation (reviewed by Laue et al., 1992) with a Beckman XL-A Optima Analytical Ultracentrifuge equipped with absorbance optics. A Beckman An-60Ti rotor was used at 22,000 and 27,000 rpm. Experiments were performed at pH 7.2 and pH 4.7. LOOP-36 samples were made at three concentrations (300, 100, and 33 μM) per pH, and LOOP-52 samples also were made at three concentrations (500, 167, and 56 μM) per pH. All samples were dialyzed exhaustively (~ 24 hr) against buffer prior to the experiments. Buffer conditions were 150 mM sodium chloride, 50 mM sodium phosphate (pH 7.2) or 150 mM sodium chloride, 5 mM sodium acetate (pH 4.7). The molecular weights were determined by a simultaneous fit of each data set using a nonlinear least squares fit algorithm, HID-4000 (Johnson et al., 1981); no systematic residuals were observed.

Acknowledgments

References

Braakman, I., Helenius, J., and Helenius, A. (1992). Role of ATP and disulphide bonds during protein folding in the endoplasmic reticulum. Nature 356, 260–262.

Brand, C. M., and Skehel, J. J. (1972). Crystalline antigen from the influenza virus envelope. Nature New Biol. 238, 145–147.

Chambers, P., Pringle, C. R., and Easton, A. J. (1990). Heptad repeat sequences are located adjacent to hydrophobic regions in several types of virus fusion glycoproteins. J. Gen. Virol. 71, 3075–3080.

Chen, Y.-H., Yang, J. T., and Chau, K. H. (1974). Determination of the helix and β form of proteins in aqueous solution by circular dichroism. Biochemistry 13, 3350–3359.

Cohen, C., and Parry, D. A. D. (1990). α-Helical coiled coils and bundles: how to design an α-helical protein. Proteins 7, 1–15.

Copeland, C. S., Doms, R. W., Bolzau, E. M., Webster, R. G., and Helenius, A. (1986). Assembly of influenza hemagglutinin trimers and its role in intracellular transport. J. Cell Biol. 103, 1179–1191.

Crick, F. H. C. (1953). The packing of α-helices: simple coiled coils. Acta Cryst. 6, 689–697.

Daniels, R. S., Downie, J. C., Hay, A. J., Knossow, M., Skehel, J. J., Wang, M. L., and Wiley, D. C. (1985). Fusion mutants of the influenza virus hemagglutinin glycoprotein. Cell 40, 431–439.

Doms, R. W., and Helenius, A. (1986). Quaternary structure of influenza virus hemagglutinin after acid treatment. J. Virol. 60, 833–839.

Doms, R. W., Helenius, A., and White, J. (1985). Membrane fusion activity of the influenza virus hemagglutinin. J. Biol. Chem. 260, 2973–2981.

Edelhoch, H. (1967). Spectroscopic determination of tryptophan and tyrosine in proteins. Biochemistry 6, 1948–1954.

Ellenberger, T. E., Brandl, C. J., Struhl, K., and Harrison, S. C. (1992). The GCN4 basic region leucine zipper binds DNA as a dimer of uninterrupted α helices: crystal structure of the protein–DNA complex. Cell 71, 1223–1237.

Fields, C. G., Lloyd, D. H., Macdonald, R. L., Otteson, K. M., and Noble, R. L. (1991). HBTU activation for automated Fmoc solid-phase peptide synthesis. Peptide Res. 4, 95–101.

Gething, M.-J., Doms, R. W., York, D., and White, J. (1986a). Studies on the mechanism of membrane fusion: site specific mutagenesis of the hemagglutinin of influenza virus. J. Cell Biol. 102, 11–23.

Gething, M.-J., McCammon, K., and Sambrook, J. (1986b). Expression of wild-type and mutant forms of influenza hemagglutinin: the role of folding in intracellular transport. Cell 46, 939–950.

Glick, G. D., Toogood, P. L., Wiley, D. C., Skehel, J. J., and Knowles, J. R. (1991). Ligand recognition by influenza virus. J. Biol. Chem. 266, 23660–23669.

Godley, L., Pfeifer, J., Steinhauer, D., Ely, B., Shaw, G., Kaufmann, R., Suchanek, E., Pabo, C., Skehel, J. J., Wiley, D. C., and Wharton, S. (1992). Introduction of intersubunit disulfide bonds in the membrane-distal region of the influenza hemagglutinin abolishes membrane fusion activity. Cell 68, 635–645.

Hodges, R. S., Sodek, J., Smillie, L. B., and Jurasek, L. (1972). Tropomyosin: amino acid sequence and coiled-coil structure. Cold Spring Harbor Symp. Quant. Biol. 37, 299–310.

Hodges, R. S., Saund, A. K., Chong, P. C. S., St.-Pierre, S. A., and Reid, R. E. (1981). Synthetic model for two-stranded α-helical coiled-coils. J. Biol. Chem. 256, 1214–1224.

Johnson, M. L., Correia, J. J., Yphantis, D. A., and Halvorson, H. R. (1981). Analysis of data from the analytical ultracentrifuge by nonlinear least-squares techniques. Biophys. J. 36, 575–588.

Kemble, G. W., Bodian, D. L., Rosé, J., Wilson, I. A., and White,

J. M. (1992). Intermonomer disulphide bonds impair the fusion activity of influenza virus hemagglutinin. J. Virol. 66, 4940–4950.

Kilbourne, E. D. (1969). Future influenza vaccines and the use of genetic recombinants. Bull. World Health Org. 41, 643–645.

Kim, P. S., and Baldwin, R. L. (1990). Intermediates in the folding reactions of small proteins. Annu. Rev. Biochem. 59, 631–660.

Klenk, H.-D., Rott, R., Orlich, M., and Blödorn, J. (1975). Activation of influenza A virus by trypsin treatment. Virology 68, 426–439.

Landschulz, W. H., Johnson, P. F., and McKnight, S. L. (1988). The leucine zipper: a hypothetical structure common to a new class of DNA binding proteins. Science 240, 1759–1764.

Laue, T. M., Shah, B. D., Ridgeway, T. M., and Pelletier, S. L. (1992). Computer-aided interpretation of analytical sedimentation data for proteins. In Analytical Ultracentrifugation in Biochemistry and Polymer Science, S. E. Harding, A. J. Rowe, and J. C. Horton, eds. (Cambridge: Royal Society of Chemistry), pp. 90–125.

Lazarowitz, S. G., and Choppin, P. W. (1975). Enhancement of the infectivity of influenza A and B viruses by proteolytic cleavage of the hemagglutinin polypeptide. Virology 68, 440–454.

Lazarowitz, S. G., Compans, R. W., and Choppin, P. W. (1971). Influenza virus structural and nonstructural proteins in infected cells and their plasma membranes. Virology 46, 830–843.

Lupas, A., Van Dyke, M., and Stock, J. (1991). Predicting coiled coils from protein sequences. Science 252, 1162–1164.

McLachlan, A. D., and Stewart, M. (1975). Tropomyosin coiled-coil interactions: evidence for an unstaggered structure. J. Mol. Biol. 98, 293–304.

Mottonen, J., Strand, A., Symersky, J., Sweet, R. M., Danley, D. E., Geoghegan, K. F., Gerard, R. D., and Goldsmith, E. J. (1992). Structural basis of latency in plasminogen activator inhibitor-1. Nature 355, 270–273.

O'Shea, E. K., Rutkowski, R., and Kim, P. S. (1989). Evidence that the leucine zipper is a coiled coil. Science 243, 538–542.

O'Shea, E. K., Klemm, J. D., Kim, P. S., and Alber, T. (1991). X-ray structure of the GCN4 leucine zipper, a two-stranded, parallel, coiled coil. Science 254, 539–544.

O'Shea, E. K., Rutkowski, R., and Kim, P. S. (1992). Mechanism of specificity in the Fos–Jun oncoprotein heterodimer. Cell 68, 699–708.

Parry, D. A. D. (1982). Coiled-coils in α-helix-containing proteins: analysis of the residue types within the heptad repeat and the use of these data in the prediction of coiled-coils in other proteins. Biosci. Rep. 2, 1017–1024.

Pauling, L., and Corey, R. B. (1953). Compound helical configurations of polypeptide chains: structure of proteins of the α-keratin type. Nature 171, 59–61.

Perez, L. G., O'Donnell, M. A., and Stephens, E. B. (1992). The transmembrane glycoprotein of human immunodeficiency virus type 1 induces syncytium formation in the absence of the receptor binding glycoprotein. J. Virol. 66, 4134–4143.

Puri, A., Booy, F. P., Doms, R. W., White, J. M., and Blumenthal, R. (1990). Conformational changes and fusion activity of influenza virus hemagglutinin of the H2 and H3 subtypes: effects of acid pretreatment. J. Virol. 64, 3824–3832.

Rabindran, S. K., Haroun, R. I., Clos, J., Wisniewski, J., and Wu, C. (1993). Regulation of heat shock factor trimer formation: role of a conserved leucine zipper. Science 259, 230–234.

Ruigrok, R. W. H., Martin, S. R., Wharton, S. A., Skehel, J. J., Bayley, P. M., and Wiley, D. C. (1986). Conformational changes in the hemagglutinin of influenza virus which accompany heat-induced fusion of virus with liposomes. Virology 155, 484–497.

Ruigrok, R. W. H., Aitken, A., Calder, L. J., Martin, S. R., Skehel, J. J., Wharton, S. A., Weis, W., and Wiley, D. C. (1988). Studies on the structure of the influenza virus hemagglutinin at the pH of membrane fusion. J. Gen. Virol. 69, 2785–2795.

Sauter, N. K., Glick, G. D., Crowther, R. L., Park, S.-J., Eisen, M. B., Skehel, J. J., Knowles, J. R., and Wiley, D. C. (1992). Crystallographic detection of a second ligand binding site in influenza virus hemagglutinin. Proc. Natl. Acad. Sci. USA 89, 324–328.

Skehel, J. J., and Waterfield, M. D. (1975). Studies on the primary structure of the influenza virus hemagglutinin. Proc. Natl. Acad. Sci. USA 72, 93–97.

Skehel, J. J., Bayley, P. M., Brown, E. B., Martin, S. R., Waterfield, M. D., White, J. M., Wilson, I. A., and Wiley, D. C. (1982). Changes in the conformation of influenza virus hemagglutinin at the pH optimum of virus-mediated membrane fusion. Proc. Natl. Acad. Sci. USA 79, 968–972.

Stegmann, T., and Helenius, A. (1993). Influenza virus fusion: from models toward a mechanism. In Viral Fusion Mechanisms, J. Bentz, ed. (Boca Raton, Florida: CRC Press), pp. 89–111.

Stegmann, T., White, J. M., and Helenius, A. (1990). Intermediates in influenza induced membrane fusion. EMBO J. 9, 4231–4241.

Stegmann, T., Delfino, J. M., Richards, F. M., and Helenius, A. (1991). The HA2 subunit of influenza hemagglutinin inserts into the target membrane prior to fusion. J. Biol. Chem. 266, 18404–18410.

Stein, P. E., Leslie, A. G. W., Finch, J. T., Turnell, W. G., McLaughlin, P. J., and Carrell, R. W. (1990). Crystal structure of ovalbumin as a model for the reactive centre of serpins. Nature 347, 99–102.

Vaishnav, Y. N., and Wong-Staal, F. (1991). The biochemistry of AIDS. Annu. Rev. Biochem. 60, 577–630.

Ward, C. W., and Dopheide, T. A. (1980). Influenza virus hemagglutinin. Structural predictions suggest that the fibrillar appearance is due to the presence of a coiled-coil. Aust. J. Biol. Sci. 33, 441–447.

Weis, W., Brown, J. H., Cusack, S., Paulson, J. C., Skehel, J. J., and Wiley, D. C. (1988). Structure of the influenza virus haemagglutinin complexed with its receptor, sialic acid. Nature 333, 426–431.

Weis, W. I., Brünger, A. T., Skehel, J. J., and Wiley, D. C. (1990a). Refinement of the influenza virus hemagglutinin by simulated annealing. J. Mol. Biol. 212, 737–761.

Weis, W. I., Cusack, S. C., Brown, J. H., Daniels, R. S., Skehel, J. J., and Wiley, D. C. (1990b). The structure of a membrane fusion mutant of the influenza virus haemagglutinin. EMBO J. 9, 17–24.

Wharton, S. A., Skehel, J. J., and Wiley, D. C. (1986). Studies of influenza haemagglutinin-mediated membrane fusion. Virology 149, 27–35.

White, J. M. (1990). Viral and cellular membrane fusion proteins. Annu. Rev. Physiol. 52, 675–697.

White, J. M. (1992). Membrane fusion. Science 258, 917–924.

White, J. M., and Wilson, I. A. (1987). Anti-peptide antibodies detect steps in a protein conformational change: low-pH activation of the influenza virus hemagglutinin. J. Cell Biol. 105, 2887–2896.

White, J., Helenius, A., and Gething, M.-J. (1982a). Haemagglutinin of influenza virus expressed from a cloned gene promotes membrane fusion. Nature 300, 658–659.

White, J., Kartenbeck, J., and Helenius, A. (1982b). Membrane fusion activity of influenza virus. EMBO J. 1, 217–222.

Wild, C., Oas, T., McDanal, C., Bolognesi, D., and Matthews, T. (1992). A synthetic peptide inhibitor of human immunodeficiency virus replication: correlation between solution structure and viral inhibition. Proc. Natl. Acad. Sci. USA 89, 10537–10541.

Wiley, D. C., and Skehel, J. J. (1987). The structure and function of the hemagglutinin membrane glycoprotein of influenza virus. Annu. Rev. Biochem. 56, 365–394.

Wilson, I. A., Skehel, J. J., and Wiley, D. C. (1981). Structure of the haemagglutinin membrane glycoprotein of influenza virus at 3 Å resolution. Nature 289, 366–373.

Woody, R. W. (1985). Circular dichroism of peptides. In The Peptides, Volume 7, S. Udenfriend, J. Meienhofer, and V. J. Hruby, eds. (Orlando, Florida: Academic Press, Inc.), pp. 15–114.

Wright, H. T., Qian, H. X., and Huber, R. (1990). Crystal structure of plakalbumin, a proteolytically nicked form of ovalbumin. J. Mol. Biol. 213, 513–528.

Wright, P. E., Dyson, J., and Lerner, R. A. (1988). Conformation of peptide fragments of proteins in aqueous solution: implications for initiation of protein folding. Biochemistry 27, 7167–7175.

Note Added In Proof

Recently, a connection was made between fusion proteins involved in cellular vesicle transport and vesicle–synaptosomal membrane fusion (Söllner, T., Whiteheart, S. W., Brunner, M., Erdjument-Bromage, H., Geromanos, S., Tempst, P., and Rothman, J. E. (1993). SNAP receptors implicated in vesicle targeting and fusion. Nature 362, 318–324). The amino acid sequences for some of these membrane proteins contain a long, continuous region of 4-3 hydrophobic repeats.